Coupled-channel method for nuclear scattering of Dirac particles: High-energy electrons on calcium*

Robert L. Mercer

Speech-Processing Group, Computer Science Department, International Business Machines Corporation, Thomas J. Watson Research Center, Yorktown Heights, New York 10598

(Received 18 August 1976)

We obtain a solution of the Dirac equation in the presence of the electromagnetic field of a complex nucleus by means of coupled-channel partial wave analysis using a new method in which the asymptotic solutions of the coupled radial wave equations include all electromagnetic couplings. A computer program employing this method is used to determine the importance of dispersion effects in the scattering of 250 MeV electrons from ^{40}Ca and ^{44}Ca. We find the dispersion effects to be less than 1% for angles below 90° (i.e., considerably less than experimental error over the range investigated experimentally), thus supporting the view that the difference in the differential cross sections from ^{40}Ca and ^{44}Ca arises primarily from a difference in the ground state charge distributions of the two isotopes.

[NUCLEAR REACTIONS ^{40}Ca(e,e'), ^{44}Ca(e,e'), $E=250$ MeV, $E=50$ MeV, calculations; coupled-channel calculation of dispersion effects; energy dependence of dispersion effects.]

I. INTRODUCTION

There arises, in the course of analyzing high energy electron-nucleus scattering experiments, the problem of determining the differential cross section given a particular charge distribution for the scattering target.[1] Computer codes which perform this type of analysis by means of the partial wave method have been available for many years.[2,3] These codes, which are able to handle single-channel scattering, are adequate to the extent that the nucleus may be approximated by a static, spherically symmetric charge distribution. Therefore they have found their most fruitful applications in analyses of electron scattering from doubly or singly magic nuclei in which there are no low-lying excited states.

As the need arose to analyze data from more complex nuclei, the distorted wave Born approximation (DWBA), in which the distortion of the incoming plane wave by the Coulomb field surrounding the nucleus is correctly accounted for by the partial wave method, and nuclear distortions, etc., are treated as first-order perturbations, was employed. In some cases, however, the DWBA treatment is inadequate.

A proper treatment of the higher order effects of excited states and of higher multipole fields requires a complete coupled-channel partial wave analysis of the Dirac equation. For bound states, this problem was first solved by McKinley[4] in the course of determining the eigenvalues of muonic atoms. The scattering problem is more difficult because the wave functions extend throughout all space. We present here a computational solution to the coupled-channel problem for a Dirac particle scattering from a complex nucleus. The coupled radial wave equations are integrated from the origin to the edge of the nucleus using a standard multistep integration technique, from which point they are carried on by analytic continuation with successive power series expansions to a radius at which the asymptotic solutions of the coupled radial wave equations converge sufficiently for an adequate determination of the partial wave phase shifts. The asymptotic solutions themselves include all electromagnetic couplings and thus may be used at much smaller radii than solutions such as the standard, relativistic Coulomb wave functions which include only monopole potentials. Our solution is embodied in the computer program ZENITH which is written in IBM FORTRAN IV and currently runs on IBM System/360 and System/370 equipment. Results obtained with ZENITH have been published elsewhere.[5-7] Recently, Saladin, Roesel, and Alder[8] have suggested a method quite similar to ours for analyzing Coulomb excitation experiments with the Schrödinger equation.

In Sec. II, we develop the partial wave formalism and derive an asymptotic solution to the resulting coupled radial wave equations. In Sec. III, we determine the matrix elements of the electromagnetic interaction. Section IV deals with several numerical procedures employed in ZENITH, and in Sec. V we discuss a number of tests which have been made to ensure proper operation. In Sec. VI, the program is applied to determine the importance of dispersion effects in the scattering of 250 MeV electrons from ^{40}Ca and ^{44}Ca. We find the dispersion effects to be less than 1% for angles below 90° (i.e., considerably less than experimental error over the range investigated experimentally),

thus supporting the view that the difference in the differential cross sections from ^{40}Ca and ^{44}Ca arises primarily from a difference in the ground state charge distributions of the two isotopes.[9] Section VII is a brief summary and discussion.

This paper is essentially a condensed version of the author's Ph.D. thesis,[10] from which additional details may be obtained in many cases.

II. PARTIAL WAVE FORMALISM

The wave function $\Psi(\vec{r})$ for a free Dirac particle of mass m with total energy E is a four-component spinor satisfying the wave equation[11]

$$H_D\Psi(\vec{r}) = (-i\vec{\alpha}\cdot\vec{\nabla} + \beta m)\Psi(\vec{r}) = E\Psi(\vec{r}) .$$

The Dirac matrices α and β are 4 by 4 matrices operating on the components of $\Psi(\vec{r})$. They are defined by

$$\vec{\alpha} = \begin{pmatrix} 0 & \vec{\sigma} \\ \vec{\sigma} & 0 \end{pmatrix}, \quad \beta = \begin{pmatrix} I & 0 \\ 0 & -I \end{pmatrix},$$

where I is the 2 by 2 unit matrix and the components of $\vec{\sigma} = (\sigma_1, \sigma_2, \sigma_3)$ are the Pauli spin matrices. The total angular momentum operator is the sum of an orbital part and a spin part:

$$\vec{J} = \vec{L} + \vec{S} = -i\vec{r}\times\vec{\nabla} + \frac{1}{2}\begin{pmatrix} \vec{\sigma} & 0 \\ 0 & \vec{\sigma} \end{pmatrix} .$$

Given eigenstates $|LM\rangle$ of $\vec{L}^2$ and L_3 with eigenvalues $L(L+1)$ and M, respectively, together with eigenstates $|\frac{1}{2}M_s\rangle$ of $(\frac{1}{2}\vec{\sigma})^2$, and $\frac{1}{2}\sigma_3$ with eigenvalues $\frac{3}{4}$ and M_s, respectively, we construct eigenstates $|JL\mu\rangle$ of $(\vec{L}+\frac{1}{2}\vec{\sigma})^2$, $\vec{L}^2$, and $L_3+\frac{1}{2}\sigma_3$ with eigenvalues $J(J+1)$, $L(L+1)$, and μ, respectively. These are the spinor spherical harmonics. We have[12]

$$|JL\mu\rangle = \sum_{MM_s} C^{L\frac{1}{2}J}_{MM_s\mu}\,|LM\rangle|\tfrac{1}{2}M_s\rangle .$$

To each value of J, there correspond two possible values of L: $L = J - \frac{1}{2}$ and $L = J + \frac{1}{2}$. Consequently, J and L may be combined into a single quantum number χ as follows:

$$\chi(J,L) = 2(L-J)(J+\tfrac{1}{2}) ,$$

$$J(\chi) = |\chi| - \tfrac{1}{2} ,$$

$$L(\chi) = J(\chi) + \tfrac{1}{2}\,\mathrm{sgn}\chi .$$

Hereafter, χ and the pair J, L will be used interchangeably without explicitly illustrating the dependence of one upon the other. We will frequently identify the ket $|LM\rangle$ with the spherical harmonic $i^L Y_{LM}(\theta\phi) = \langle\theta\phi|LM\rangle$. This choice of phases is unimportant for monopole scattering but is a great convenience for more general scattering situations. The spinor spherical harmonics form an orthonormal basis for the space spanned by the kets $|LM\rangle|\frac{1}{2}M_s\rangle$.

Consider, now, the scattering of a Dirac particle of mass m and charge ze from an infinitely massive nucleus of charge Ze. Let the Hamiltonian governing the internal state of the nucleus be H_N and let the interaction between the nucleus and the Dirac particle be $V(\vec{r})$. The wave function $\Psi(\vec{r})$ then satisfies the wave equation

$$[H_D + V(\vec{r}) + H_N]\Psi(\vec{r}) = E\Psi(\vec{r}) . \tag{1}$$

In terms of the variable $\vec{r}$, Eq. (1) represents a set of coupled linear partial differential equations. The partial wave method exploits the invariance of Eq. (1) under spatial rotations and reflections to replace it with an infinite collection of sets of coupled ordinary differential equations in the radial variable $r = |\vec{r}|$. We will be interested primarily in the case where $V(\vec{r})$ is the electromagnetic interaction, which we write in the form

$$V(\vec{r}) = S(\vec{r}) + \vec{V}(\vec{r})\cdot\vec{\alpha} .$$

Let $\vec{I}$ and P_N be the angular momentum and parity operators of the nucleus. We choose as a basis for the state space of the nucleus, the kets $|nM\rangle$, $0 \leq n \leq N-1$, and $-I_n \leq M \leq I_n$, which are simultaneous eigenstates of H_N, $\vec{I}^2$, I_3, and P_N with eigenvalues ϵ_n, $I_n(I_n+1)$, M, and p_n, respectively. The wave function may be written as a series of the form

$$\Psi(\vec{r}) = \sum_{st} a_s r^{-1}\begin{pmatrix} g^{st}(r)\,|t\rangle \\ f^{st}(r)\,|t\rangle \end{pmatrix} ,$$

where the kets $|t\rangle$ form a basis for the space spanned by the kets $|nM\rangle|\chi\mu\rangle$. The total angular momentum operator for Eq. (1) is $\vec{F} = \vec{J} + \vec{I}$, and the total parity operator is $P = P_D P_N$ where P_D is the parity operator for the Dirac particle. The kets $|t\rangle$ may be chosen to be simultaneous eigenstates of the operators $\vec{F}^2$, F_3, and P, when these operators are restricted to either the upper or the lower components of the Dirac spinor. One such set of eigenstates is

$$|fm_f p\chi n\rangle = \sum_{\mu M} C^{JIf}_{\mu M m_f}\,|\chi\mu\rangle|nM\rangle \tag{2}$$

for which $p = p_n(-1)^L$. In general, to a pair of eigenvalues f and p, there correspond several possible pairs (χ, n). Let $N(f,p)$ be the set of such pairs and let $\mathfrak{N}(f,p)$ be its cardinality. It is clear that if $(\chi,n)\in N(f,p)$ then $(-\chi,n)\in N(f,-p)$. As a notational convenience, we introduce a single quantum number, say j, such that as j ranges from 1 to $\mathfrak{N}(f,p)$, (χ_j, n_j) ranges over all of the pairs in $N(f,p)$. If j is the quantum number corresponding to the pair (χ,n) in $N(f,p)$, let j_- be that corresponding to the pair $(-\chi,n)$ in $N(f,-p)$.

We now express $\Psi(\vec{r})$ in the form

$$\Psi(\vec{r}) = \sum_{\substack{f m_f p \\ ij}} a^i_{f m_f p} r^{-1} \begin{pmatrix} g^{ij}_{fp}(r)\,|\,f m_f p j\rangle \\ -\mathrm{sgn}\chi_j f^{ij}_{fp}(r)\,|\,f m_f - p j_-\rangle \end{pmatrix}. \tag{3}$$

Upon substituting this expression into Eq. (1) and making use of the form we have assumed for $V(\vec{r})$, we obtain, in terms of the dimensionless quantities $\rho = Er$, $\tau = mE^{-1}$, and $t_n = 1 - \epsilon_n E^{-1}$, the differential equations

$$\begin{aligned} &\left(\frac{d}{d\rho} - \frac{\chi_j}{\rho}\right) f^{ij}_{fp}(\rho) + (t_{n_j} - \tau) g^{ij}_{fp}(\rho) = \sum_k [s^f_{jk}(\rho) g^{ik}_{fp}(\rho) - v^f_{jk}(\rho) f^{ik}_{fp}(\rho)], \\ &\left(\frac{d}{d\rho} + \frac{\chi_j}{\rho}\right) g^{ij}_{fp}(\rho) - (t_{n_j} + \tau) f^{ij}_{fp}(\rho) = -\sum_k \mathrm{sgn}\chi_j \cdot \chi_k [s^f_{j_- k_-}(\rho) f^{ik}_{fp}(\rho) + v^f_{j_- k_-}(\rho) g^{ik}_{fp}(\rho)], \end{aligned} \tag{4}$$

in which

$$s^f_{jk}(\rho) = \langle f m_f p j \,|\, S(\vec{r}) E^{-1} \,|\, f m_f p k\rangle \quad \text{and} \quad v^f_{jk}(\rho) = \langle f m_f p j \,|\, \mathrm{sgn}\chi_k \vec{V}(\vec{r}) \cdot \vec{\sigma} E^{-1} \,|\, f m_f - p k_-\rangle .$$

The index i in the equations above distinguishes among the $\mathfrak{N}(f,p)$ independent regular solutions whose behavior near the origin is given by

$$\lim_{\rho\to 0} [f^{ij}_{fp}(\rho)\rho^{-|\chi_j|}] = \delta_{ij}, \quad \lim_{\rho\to 0} [g^{ij}_{fp}(\rho)\rho^{-|\chi_j|}] = 0, \quad \chi_i > 0;$$

$$\lim_{\rho\to 0} [f^{ij}_{fp}(\rho)\rho^{-|\chi_j|}] = 0, \quad \lim_{\rho\to 0} [g^{ij}_{fp}(\rho)\rho^{-|\chi_j|}] = \delta_{ij}, \quad \chi_i < 0.$$

Asymptotically,

$$s^f_{jk}(\rho) \underset{\rho\to\infty}{\sim} \sum_{\lambda=0}^{L} \alpha^{f\lambda}_{jk} \rho^{-\lambda-1} \quad \text{and} \quad v^f_{jk}(\rho) \underset{\rho\to\infty}{\sim} \sum_{\lambda=0}^{L} \beta^{f\lambda}_{jk} \rho^{-\lambda-1}, \tag{5}$$

in which $\alpha^{f\lambda}_{jk}$, and $\beta^{f\lambda}_{jk}$, are independent of ρ. In particular, $\alpha^{f0}_{jk} = -\gamma\delta_{jk}$ and $\beta^{f0}_{jk} = 0$, where $\gamma = zZe^2$. When all of the constants $\alpha^{f\lambda}_{jk}$ and $\beta^{f\lambda}_{jk}$ are zero for $\lambda \geq 1$, Eqs. (4) decouple asymptotically into $\mathfrak{N}(f,p)$ pairs of relativistic Coulomb wave equations which may be solved easily. When some of the constants $\alpha^{f\lambda}_{jk}$ and $\beta^{f\lambda}_{jk}$ are nonzero for $\lambda \geq 1$, Eqs. (4) do not decouple asymptotically. In place of the relativistic Coulomb wave equations, we are faced with the differential equations

$$\begin{aligned} &\left(\frac{d}{d\rho} - \frac{\chi_j}{\rho}\right) F^{ij}_{fp}(\rho) + (t_{n_j} - \tau) G^{ij}_{fp}(\rho) = \sum_{\lambda=0}^{L} \sum_k \rho^{-\lambda-1} [\alpha^{f\lambda}_{jk} G^{ik}_{fp}(\rho) - \beta^{f\lambda}_{jk} F^{ik}_{fp}(\rho)], \\ &\left(\frac{d}{d\rho} + \frac{\chi_j}{\rho}\right) G^{ij}_{fp}(\rho) - (t_{n_j} + \tau) F^{ij}_{fp}(\rho) = -\sum_{\lambda=0}^{L} \sum_k \rho^{-\lambda-1} \mathrm{sgn}\chi_j \cdot \chi_k [\alpha^{f\lambda}_{j_- k_-} F^{ik}_{fp}(\rho) + \beta^{f\lambda}_{j_- k_-} G^{ik}_{fp}(\rho)]. \end{aligned} \tag{6}$$

These equations have a nasty singularity at the origin and the analytic methods which are successful in the Coulomb case avail us nothing here.

It is possible, however, to obtain an expansion for the solutions of Eqs. (6) which is valid as ρ tends to infinity. In obtaining this expansion we drop the indices f and p. We write

$$F^{ij}(\rho) = \sum_{m=0}^{\infty} [\sin(k_i\rho + \gamma t_i k_i^{-1} \ln 2k_i\rho - L_i\pi/2) s^{(m)}_{ij} + \cos(k_i\rho + \gamma t_i k_i^{-1} \ln 2k_i\rho - L_i\pi/2) t^{(m)}_{ij}]\rho^{-m},$$

$$G^{ij}(\rho) = \sum_{m=0}^{\infty} [\sin(k_i\rho + \gamma t_i k_i^{-1} \ln 2k_i\rho - L_i\pi/2) u^{(m)}_{ij} + \cos(k_i\rho + \gamma t_i k_i^{-1} \ln 2k_i\rho - L_i\pi/2) v^{(m)}_{ij}]\rho^{-m},$$

where the dimensionless wave number k_i equals $(t_i^2 - \tau^2)^{1/2}$. (Note that k, t, and L depend on the first superscript associated with F and G, which is the one enumerating sets of independent solutions.) If we introduce these expansions into Eqs. (6) and equate the coefficients of $\sin(\ldots)\rho^{-m}$ and $\cos(\ldots)\rho^{-m}$ in the resulting expressions to zero, we obtain recursion relations for the unknown constants $s^{(m)}_{ij}$, $t^{(m)}_{ij}$, $u^{(m)}_{ij}$, and $v^{(m)}_{ij}$. Let

$$A_{ij}=\begin{bmatrix} 0 & -k_i & t_j-\tau & 0 \\ k_i & 0 & 0 & t_j-\tau \\ -t_j-\tau & 0 & 0 & -k_i \\ 0 & -t_j-\tau & k_i & 0 \end{bmatrix}, \quad M_{ij}^{(m)}=\begin{bmatrix} \chi_j+m-1 & \gamma t_i k_i^{-1} & -\gamma & 0 \\ -\gamma t_i k_i^{-1} & \chi_j+m-1 & 0 & -\gamma \\ \gamma & 0 & -\chi_j+m-1 & \gamma t_i k_i^{-1} \\ 0 & \gamma & -\gamma t_i k_i^{-1} & -\chi_j+m-1 \end{bmatrix},$$

$$C_{jk}^{(\lambda)}=\begin{bmatrix} -\mathrm{sgn}\chi_j\beta_{jk}^{(\lambda)} & 0 & \mathrm{sgn}\chi_j\alpha_{jk}^{(\lambda)} & 0 \\ 0 & -\mathrm{sgn}\chi_j\beta_{jk}^{(\lambda)} & 0 & \mathrm{sgn}\chi_j\alpha_{jk}^{(\lambda)} \\ -\mathrm{sgn}\chi_k\alpha_{j_-k_-}^{(\lambda)} & 0 & -\mathrm{sgn}\chi_k\beta_{j_-k_-}^{(\lambda)} & 0 \\ 0 & -\mathrm{sgn}\chi_k\alpha_{j_-k_-}^{(\lambda)} & 0 & -\mathrm{sgn}\chi_k\beta_{j_-k_-}^{(\lambda)} \end{bmatrix}.$$

Then if

$$S_{ij}^{(m)}=\begin{bmatrix} s_{ij}^{(m)} \\ t_{ij}^{(m)} \\ u_{ij}^{(m)} \\ v_{ij}^{(m)} \end{bmatrix},$$

we have

$$A_{ij}S_{ij}^{(m)}=M_{ij}^{(m)}S_{ij}^{(m-1)}+\sum_{\lambda=1}^{L}\sum_{k}C_{jk}^{(\lambda)}S_{ik}^{(m-\lambda-1)}. \tag{7}$$

Let

$$B_{ij}=\begin{bmatrix} 0 & k_i & t_j-\tau & 0 \\ -k_i & 0 & 0 & t_j-\tau \\ -t_j-\tau & 0 & 0 & k_i \\ 0 & -t_j-\tau & -k_i & 0 \end{bmatrix}.$$

If we multiply both sides of Eq. (7) on the left by B_{ij} then we have

$$(k_i^2-k_j^2)S_{ij}^{(m)}=B_{ij}M_{ij}^{(m)}S_{ij}^{(m-1)}+\sum_{\lambda=1}^{L}\sum_{k}B_{ij}C_{jk}^{(\lambda)}S_{ik}^{(m-\lambda-1)}. \tag{8}$$

When $k_i\neq k_j$, we can divide Eq. (8) by $(k_i^2-k_j^2)$ to obtain the desired recursion relation.[13] When $k_i=k_j$, we can replace m in Eq. (8) by $m+1$ and add the resulting equation to Eq. (7) to obtain

$$(A_{ij}+B_{ij}M_{ij}^{(m+1)})S_{ij}^{(m)}=M_{ij}^{(m)}S_{ij}^{(m-1)}+\sum_{\lambda=1}^{L}\sum_{k}(C_{jk}^{(\lambda)}S_{ik}^{(m-\lambda-1)}-B_{ij}C_{jk}^{(\lambda)}S_{ik}^{(m-\lambda)}). \tag{9}$$

If we write $k_i=k_j=k$, $t_i=t_j=t$, and $t\pm\tau=t_\pm$, then after considerable algebra one may verify that

$$(A_{ij}+B_{ij}M_{ij}^{(m+1)})^{-1}=(4k^2m)^{-1}\begin{bmatrix} \tau\gamma & k(m-1-\chi_j) & -t_-(m+1-\chi_j) & \tau\gamma t_-k^{-1} \\ -k(m-1-\chi_j) & \tau\gamma & -\tau\gamma t_-k^{-1} & -t_-(m+1-\chi_j) \\ t_+(m+1+\chi_j) & \tau\gamma t_+k^{-1} & -\tau\gamma & k(m-1+\chi_j) \\ -\tau\gamma t_+k^{-1} & t_+(m+1+\chi_j) & -k(m-1+\chi_j) & -\tau\gamma \end{bmatrix}.$$

Thus Eq. (9) yields a usable recursion relation whenever A_{ij} is singular and $m\neq 0$.

Finally, when $m=0$, Eq. (7) gives us the following condition on $S_{ij}^{(0)}$:

$$A_{ij}S_{ij}^{(0)}=0.$$

If A_{ij} is nonsingular, this simply states that $S_{ij}^{(0)}=0$, but when A_{ij} is singular there are nontrivial choices of $S_{ij}^{(0)}$ which can be made. In fact, there are two linearly independent solutions which may be taken as the first two columns of B_{ij}. Altogether, there are $2\mathfrak{N}(f,p)$ sets of independent solu-

tions to Eqs. (6). We distinguish among them according to their asymptotic behavior as follows:

$$G_R^{ij}(\rho) \underset{\rho\to\infty}{\sim} \sin(k_i\rho+\gamma t_i k_i^{-1}\ln 2k_i\rho - L_i\pi/2)\delta_{ij},$$

$$F_R^{ij}(\rho) \underset{\rho\to\infty}{\sim} k_i(t_i+\tau)^{-1}\cos(k_i\rho+\gamma t_i k_i^{-1}\ln 2k_i\rho - L_i\pi/2)\delta_{ij}$$

and

$$G_I^{ij}(\rho) \underset{\rho\to\infty}{\sim} \cos(k_i\rho+\gamma t_i k_i^{-1}\ln 2k_i\rho - L_i\pi/2)\delta_{ij},$$

$$F_I^{ij}(\rho) \underset{\rho\to\infty}{\sim} -k_i(t_i+\tau)^{-1}\sin(k_i\rho+\gamma t_i k_i^{-1}\ln 2k_i\rho - L_i\pi/2)\delta_{ij}.$$

Because these functions play a role in the general theory analogous to that played by the relativistic Coulomb wave functions in the single-state monopole theory, we have used the subscripts R and I indicating regular and irregular as is customary there. These subscripts do not, of course, imply anything about the behavior of these functions at the origin.

Equations (4) and (6) have the same asymptotic behavior. Therefore, we can find constants B_{fp}^{ik} and C_{fp}^{ik} such that

$$\begin{pmatrix} f_{fp}^{ij}(\rho) \\ g_{fp}^{ij}(\rho) \end{pmatrix} \underset{\rho\to\infty}{\sim} \sum_k B_{fp}^{ik}\begin{pmatrix} F_{fp,R}^{kj}(\rho) \\ G_{fp,R}^{kj}(\rho) \end{pmatrix} + C_{fp}^{ik}\begin{pmatrix} F_{fp,I}^{kj}(\rho) \\ G_{fp,I}^{kj}(\rho) \end{pmatrix}$$

or equivalently,

$$g_{fp}^{ij}(\rho) \underset{\rho\to\infty}{\sim} A_{fp}^{ij}\sin(k_j\rho+\gamma t_j k_j^{-1}\ln 2k_j\rho - L_j\pi/2+\delta_{fp}^{ij}),$$

$$f_{fp}^{ij}(\rho) \underset{\rho\to\infty}{\sim} k_j(t_j+\tau)^{-1}A_{fp}^{ij}\cos(k_j\rho+\gamma t_j k_j^{-1}\ln 2k_j\rho - L_j\pi/2+\delta_{fp}^{ij}) \qquad (10)$$

with partial wave amplitudes and phase shifts given by

$$A_{fp}^{ij} = [(C_{fp}^{ij})^2+(B_{fp}^{ij})^2]^{1/2},$$

$$\delta_{fp}^{ij} = \tan^{-1}(C_{fp}^{ij}/B_{fp}^{ij}).$$

We must now choose the coefficients $a_{fm_fp}^{i}$ in Eq. (3) to satisfy some set of boundary conditions. In particular, we wish to have $\Psi(\vec{r})$ represent the scattering of a plane wave incident along the negative z-axis. Although in the vicinity of the nucleus it is quite complicated, at great distances from the nucleus, $\Psi(\vec{r})$ must comprise a spherically outgoing scattered wave together with the incident plane wave. A plane wave itself may be written as the superposition of a spherically incoming wave and spherically outgoing wave. The appropriate boundary conditions therefore are that, asymptotically, the spherically incoming portion of $\Psi(\vec{r})$ be identical with the spherically incoming portion of a plane wave incident in the proper direction.

The wave function for a plane wave Dirac particle incident along the negative z axis may be written as

$$\Phi^{m_sM}(\vec{\rho}) = e^{ik_0\rho_z}\left(\frac{t_0+\tau}{2t_0}\right)^{1/2}\begin{pmatrix} 1 \\ \dfrac{2m_sk_0}{t_0+\tau} \end{pmatrix}|\tfrac{1}{2}m_s\rangle|0M\rangle,$$

where m_s is the spin projection of the Dirac particle along the z axis and M is that of the nucleus. We may expand $\Phi^{m_sM}(\rho)$ in spherical harmonics as follows:

$$\Phi^{m_sM}(\vec{\rho}) = \sum_{\lambda=0}[4\pi(2\lambda+1)]^{1/2}i^{\lambda}j_\lambda(k_0\rho)Y_{\lambda 0}(\theta\phi) \times\left(\frac{t_0+\tau}{2t_0}\right)^{1/2}\begin{pmatrix} 1 \\ \dfrac{2m_sk_0}{t_0+\tau} \end{pmatrix}|\tfrac{1}{2}m_s\rangle|0M\rangle$$

in which $j_\lambda(k_0\rho)$ is the regular spherical Bessel function. Asymptotically then, the spherically incoming part of $\Phi^{m_sM}(\rho)$ is

$$\Phi_{in}^{m_sM}(\vec{\rho}) = -\sum_{\lambda=0}[4\pi(2\lambda+1)]^{1/2}\frac{1}{2ik_0\rho} \times\exp[-i(k_0\rho-\lambda\pi/2)]\left(\frac{t_0+\tau}{2t_0}\right)^{1/2} \times|\lambda 0\rangle|\tfrac{1}{2}m_s\rangle|0M\rangle. \qquad (11)$$

(For simplicity, we have written only the upper components of the Dirac spinor.) Because of the long range of the Coulomb potential, it is necessary to replace Eq. (11) by

$$\Phi_{in,C}^{m_sM}(\vec{\rho}) = -\sum_{\lambda=0}[4\pi(2\lambda+1)]^{1/2}\frac{1}{2ik_0\rho} \times\exp[-i(k_0\rho+\gamma t_0k_0^{-1}\ln 2k_0\rho-\lambda\pi/2)] \times\left(\frac{t_0+\tau}{2t_0}\right)^{1/2}|\lambda 0\rangle|\tfrac{1}{2}m_s\rangle|0M\rangle \qquad (12)$$

when γ is not zero.

From Eq. (10), it is clear that the spherically incoming portion of $g_{fp}^{ij}(\rho)$ is given asymptotically by

$$g_{fp,in}^{ij}(\rho) \underset{\rho\to\infty}{\sim} -\frac{A_{fp}^{ij}}{2i}\exp[-i(k_j\rho+\gamma t_jk_j^{-1}\ln 2k_j\rho - L_j\pi/2+\delta_{fp}^{ij})]. \qquad (13)$$

Thus, we must choose the coefficients $a_{fm_fp}^{i}$ so that

$$\Phi_{in,C}^{m_s M}(\vec{\rho}) = -\sum_{\substack{f m_f p \\ ij}} a^i_{f m_f p} \frac{A^{ij}_{fp}}{2i\rho} \times \exp[-(k_j \rho + \gamma t_j k_j^{-1} \ln 2k_j \rho - L_j \pi/2 + \delta^{ij}_{fp})] | f m_f p j \rangle .$$

Multiplying this on the left by $\langle f m_f p j|$, and using Eq. (2) we find

$$\sum_i a^i_{f m_f p} A^{ij}_{fp} \exp(-i\delta^{ij}_{fp}) = [4\pi(2L_j+1)]^{1/2} k_0^{-1} \left(\frac{t_0+\tau}{2t_0}\right)^{1/2} \times C^{J_j I_j f}_{m_s M m_f} C^{L_j \frac{1}{2} J_j}_{0 m_s m_s} \delta_{0 n_j} .$$

Considered as an $\mathfrak{N}(f,p)\times\mathfrak{N}(f,p)$ matrix, $A^{ij}_{fp}\exp(-i\delta^{ij}_{fp})$ cannot be singular because the solutions g^{ij}_{fp}, f^{ij}_{fp} are independent. Let h^{ij}_{fp} be its inverse. Then

$$a^i_{f m_f p} = \sum_j [4\pi(2L_j+1)]^{1/2} k_0^{-1} \left(\frac{t_0+\tau}{2t_0}\right)^{1/2} \times h^{ji}_{fp} C^{J_j I_j f}_{m_s M m_f} C^{L_j \frac{1}{2} J_j}_{0 m_s m_s} \delta_{0 n_j} .$$

Inserting this into Eq. (3) and making use of Eq. (10), we have

$$\Psi(\vec{\rho}) \underset{\rho\to\infty}{\sim} \Phi^{m_s M}_{in,C}(\vec{\rho}) + \rho^{-1} \left(\frac{t_0+\tau}{2t_0}\right)^{1/2} \times \sum_{r M_s M_I} \exp[i(k_r \rho + \gamma t_r k_r^{-1} \ln 2k_r \rho)] \begin{pmatrix} 0 \\ \frac{\vec{\sigma}\cdot\vec{k}_r}{t_r+\tau} \end{pmatrix} \times f^{m_s M M_I M_s}_{0\to r}(\theta\phi) | \tfrac{1}{2} M_s \rangle | r M_I \rangle , \quad (14)$$

where the scattering amplitudes $f^{m_s M M_I M_s}_{0\to r}(\theta\phi)$ are given by

$$f^{m_s M M_I M_s}_{0\to r}(\theta\phi) = \sum_{\substack{fp \\ jk}} M^{jk}_{fpr} (2L_j+1)^{1/2} C^{J_j I_0 f}_{m_s M m_f} C^{L_j \frac{1}{2} J_j}_{0 m_s m_s} \times C^{J_k I_r f}_{M_J M_I m_f} C^{L_k \frac{1}{2} J_k}_{M_L M_s M_J} Y_{L_k M_L}(\theta\phi) , \quad (15)$$

with

$$M^{jk}_{fpr} = -\sum_i i\pi^{1/2} k_0^{-1} h^{ji}_{fp} A^{ik}_{fp} \exp(i\delta^{ik}_{fp}) \delta_{0 n_j} \delta_{r n_k} ,$$

and

$$M_L = m_s + M - M_I - M_s .$$

In terms of these amplitudes, the differential cross section when averaged over initial spins and summed over final spins is

$$\left(\frac{\overline{d\sigma}}{d\Omega}\right)_{0\to r} = \frac{1}{2(2I_0+1)} \left(\frac{t_r k_r}{t_r+\tau}\right) \left(\frac{t_0+\tau}{t_0 k_0}\right) \sum_{\substack{m_s M \\ M_I M_s}} |f^{m_s M M_I M_s}_{0\to r}|^2 .$$

These scattering amplitudes are not all independent. One can verify that

$$f^{-m_s -M -M_I -M_s}_{0\to r}(\theta\phi) = p_r p_0 e^{-2iM_L\phi}(-1)^{I_0 - I_r - M_L} \times f^{m_s M M_I M_s}_{0\to r}(\theta\phi) .$$

An additional simplification is possible when the mass of the scattering projectile is zero. Let $f^{ij}_{fp}(\rho,\tau)$ and $g^{ij}_{fp}(\rho,\tau)$ be the solutions of Eq. (4) and let $f^{ij}_{fp}(\rho,-\tau)$ and $g^{ij}_{fp}(\rho,-\tau)$ be the solutions of Eq. (4) when τ is replaced there by $-\tau$. Then one may establish that

$$g^{ij}_{f-p}(\rho,-\tau) = f^{ij}_{fp}(\rho,\tau) \operatorname{sgn}\chi_j ,$$

and hence that

$$A^{ij}_{f-p}(-\tau) = k_j (t_j+\tau)^{-1} A^{ij}_{fp}(\tau) ,$$

$$\delta^{ij}_{f-p}(-\tau) = \delta^{ij}_{fp}(\tau) .$$

In the limit that τ tends to zero, the ratio $k_j/(t_j+\tau)$ approaches one, and we have $A^{ij}_{f-p}(0) = A^{ij}_{fp}(0)$ and $\delta^{ij}_{f-p}(0) = \delta^{ij}_{fp}(0)$. Thus, in the zero mass limit, we need only solve Eq. (4) for one value of p. The result can then be used to determine the phase shifts and amplitudes for both values of p. One can show that under these conditions

$$f^{\frac{1}{2} M M_I -\frac{1}{2}}(\theta\phi) = e^{i\phi} \tan(\tfrac{1}{2}\theta) f^{\frac{1}{2} M M_I \frac{1}{2}}(\theta\phi) ,$$

which is physically a consequence of helicity conservation.

III. THE ELECTROMAGNETIC INTERACTION

In terms of the electromagnetic scalar and vector potentials, $\phi(\vec{r})$ and $\vec{A}(\vec{r})$, the matrix elements $s^f_{jj'}(r)$ and $v^f_{jj'}(r)$ are given by

$$s^f_{jj'}(r) = ze \langle f m_f p j | \phi(\vec{r}) | f m_f p j' \rangle \quad (16)$$

$$v^f_{jj'}(r) = ze \langle f m_f p j | \operatorname{sgn}\chi' \vec{A}(\vec{r}) \cdot \vec{\sigma} | f m_f -p j' \rangle , \quad (17)$$

where ze is the charge on the Dirac particle. We define the transition multipole potentials $\phi^{nn'}_\lambda(r)$ and $A^{nn'}_{j\lambda}(r)$ by the expansions

$$\langle nM|\phi(\vec{r})|n'M'\rangle = \sum_{\lambda\mu} (-1)^\mu C^{I'\lambda I}_{M'-\mu M} i^\lambda (2I+1)^{-1/2} \times \phi^{nn'}_\lambda(r) Y_{\lambda\mu}(\theta\phi) \quad (18)$$

and

$$\langle nM|\vec{A}(\vec{r})|n'M'\rangle = \sum_{j\lambda\mu} (-1)^\mu C^{I'\lambda I}_{M'-\mu M} i^\lambda (2I+1)^{-1/2} \times A^{nn'}_{j\lambda}(r) \vec{Y}^\mu_{j\lambda 1}(\theta\phi) . \quad (19)$$

If these expressions are substituted into Eqs. (16) and (17), then, after some algebra, we have[12]

$$s^f_{jj'}(r) = ze(-1)^{f+I-\frac{1}{2}}[(2L+1)(2L'+1)(2J+1)(2J'+1)]^{1/2} \times \sum_\lambda (-1)^{(L+\lambda-L')/2} \begin{pmatrix} L & \lambda & L' \\ 0 & 0 & 0 \end{pmatrix} \begin{Bmatrix} I' & J' & f \\ J & I & \lambda \end{Bmatrix} \begin{Bmatrix} J' & L' & \frac{1}{2} \\ L & J & \lambda \end{Bmatrix} s^{nn'}_\lambda(r) \tag{20}$$

and

$$v^f_{jj'}(r) = ze(-1)^{f+I+J+J'+\frac{1}{2}}[6(2J+1)(2J'+1)(2L+1)(2L'+1)]^{1/2} \times \sum_{j\lambda} (-1)^{j+(L+\lambda-L')/2} \begin{pmatrix} L & \lambda & L' \\ 0 & 0 & 0 \end{pmatrix} \begin{Bmatrix} I' & J' & f \\ J & I & j \end{Bmatrix} \begin{Bmatrix} L & L' & \lambda \\ J & J' & j \\ \frac{1}{2} & \frac{1}{2} & 1 \end{Bmatrix} v^{nn'}_{j\lambda}(r) . \tag{21}$$

with

$$s^{nn'}_\lambda(r) = [(2\lambda+1)/(4\pi)]^{1/2}\phi^{nn'}_\lambda(r) \tag{22}$$

and

$$v^{nn'}_{j\lambda}(r) = [(2j+1)(2\lambda+1)/(4\pi)]^{1/2}A^{nn'}_{j\lambda}(r) . \tag{23}$$

The scalar and vector potentials are generated by the nuclear charge and current densities $C(\vec{r})$ and $\vec{J}(\vec{r})$. Since we choose to work in the Coulomb gauge, $\vec{A}(\vec{r})$ is transverse and is generated by the transverse current density $\vec{J}^T(\vec{r})$. To make the scattering problem computationally tractable, we must assume the various nuclear eigenstates to be degenerate in energy. This approximation is expected, by Born-approximation arguments, to affect scattering cross sections only in the forward direction, where the momentum transfer is less than the separation of the nuclear eigenstates. This is not usually a region of experimental interest.

We may write $\vec{J}^T(\vec{r})$ as the sum of a current density and the curl of a magnetization density:

$$\vec{J}^T(\vec{r}) = \vec{J}^C(\vec{r}) + \vec{\nabla}\times\vec{\mu}(\vec{r}) . \tag{24}$$

The charge, current, and magnetization densities may be expanded in spherical harmonics as follows[14]:

$$\langle nM|C(\vec{r})|n'M'\rangle = \sum_{\lambda\mu} (-1)^\mu C^{I'\lambda I}_{M'-\mu M} i^\lambda (2I+1)^{-1/2} \times C^{nn'}_\lambda(r) Y_{\lambda\mu}(\theta\phi) , \tag{25}$$

$$\langle nM|\vec{J}^C(\vec{r})|n'M'\rangle = \sum_{\lambda\mu} (-1)^\mu C^{I'\lambda I}_{M'-\mu M} i^\lambda (2I+1)^{-1/2} \times J^{nn'}_\lambda(r)\vec{X}_{\lambda\mu}(\theta\phi) , \tag{26}$$

$$\langle nM|\vec{\mu}(\vec{r})|n'M'\rangle = \sum_{\lambda\mu} (-1)^\mu C^{I'\lambda I}_{M'-\mu M} i^\lambda (2I+1)^{-1/2} \times \mu^{nn'}_\lambda(r)\vec{X}_{\lambda\mu}(\theta\phi) . \tag{27}$$

We refer to $C^{nn'}_\lambda(r)$, $J^{nn'}_\lambda(r)$, and $\mu^{nn'}_\lambda(r)$ as the multipole charge, current, and magnetization transition densities.

Since $\vec{A}(\vec{r})$ is transverse, we may write $\vec{A}(\vec{r}) = \vec{A}^C(\vec{r}) + \vec{\nabla}\times\vec{M}(\vec{r})$ with

$$\langle nM|\vec{A}^C(\vec{r})|n'M'\rangle = \sum_{\lambda\mu} (-1)^\mu C^{I'\lambda I}_{M'-\mu M} i^\lambda (2I+1)^{-1/2} \times A^{nn'}_\lambda(r)\vec{X}_{\lambda\mu}(\theta\phi) \tag{28}$$

and

$$\langle nM|\vec{M}(\vec{r})|n'M'\rangle = \sum_{\lambda\mu} (-1)^\mu C^{I'\lambda I}_{M'-\mu M} i^\lambda (2I+1)^{-1/2} \times M^{nn'}_\lambda(r)\vec{X}_{\lambda\mu}(\theta\phi) . \tag{29}$$

It is easily established that

$$A^{nn'}_{\lambda\lambda}(r) = A^{nn'}_\lambda(r) , \tag{30}$$

$$A^{nn'}_{\lambda\lambda+1}(r) = \left(\frac{\lambda}{2\lambda+1}\right)^{1/2}\left(\frac{d}{dr} - \frac{\lambda}{r}\right)M^{nn'}_\lambda(r) , \tag{31}$$

$$A^{nn'}_{\lambda\lambda-1}(r) = -\left(\frac{\lambda+1}{2\lambda+1}\right)^{1/2}\left(\frac{d}{dr} + \frac{\lambda+1}{r}\right)M^{nn'}_\lambda(r) . \tag{32}$$

The transition multipole potentials are related to their sources by the radial equation

$$\left(\frac{1}{r^2}\frac{d}{dr}r^2\frac{d}{dr} - \frac{\lambda(\lambda+1)}{r^2}\right)[\phi_\lambda(r), A_\lambda(r), M_\lambda(r)] = -4\pi[C_\lambda(r), J_\lambda(r), \mu_\lambda(r)] . \tag{33}$$

Since the potentials are bounded at the origin and vanish at infinity, we have

$$\phi_\lambda(r) = 4\pi(2\lambda+1)^{-1}\left[r^{-\lambda-1}\int_0^r C_\lambda(x)x^{\lambda+2}dx + r^\lambda\int_r^\infty C_\lambda(x)x^{1-\lambda}dx\right] \tag{34}$$

with parallel solutions for $A_\lambda(r)$ and $M_\lambda(r)$. Thus a potential of multipolarity λ is proportional to r^λ near the origin and to $r^{-\lambda-1}$ as r tends to infinity.

IV. NUMERICAL PROCEDURES

A. Integration of the radial equations

The integration of the regular solutions of Eqs. (4) from the origin to infinity may be divided into

two regions according to the behavior of the transition potentials. Within the nucleus, the transition potentials are rather complicated functions of ρ. Beyond the edge of the nucleus, however, they are given simply by Eqs. (5). The boundary between these two regions is $\rho_{\max}$, the radius of the nucleus. The bulk of the integration from the origin to $\rho_{\max}$ is performed using Hamming's fourth-order predictor-corrector method with a step size of $\Delta\rho$. Each integration step requires one derivative evaluation plus knowledge of the functions and their derivatives at each of the four previous integration steps. The initial values of the functions and their derivatives are created by making three fourth-order Runga-Kutta steps starting with values obtained from power series expansions about the origin.

Beyond $\rho_{\max}$, Eqs. (4) reduce to Eqs. (6). The asymptotic series solutions to Eqs. (6), developed in Sec. II, will converge adequately whenever ρ is greater than, say, ρ_{asm}. When only monopole couplings are present, Eqs. (6) decouple in pairs to form sets of relativistic Coulomb wave equations. In general, however, Eqs. (6) do not decouple, and the solutions valid asymptotically cannot be related analytically to solutions in the vicinity of the origin. It is necessary to integrate Eqs. (6) from $\rho_{\max}$ to ρ_{asm} numerically.

Considered as equations with the independent variable $x=\rho-\rho_0$, Eqs. (6) have singularities at $x=-\rho_0$ and $x=\infty$. Accordingly, an expansion of the solutions in powers of x will be convergent for $|x|<\rho_0$. Let

$$F^{ij}(x)=\sum_{n=0}^{\infty} C_n^{ij} x^n,$$
$$G^{ij}(x)=\sum_{n=0}^{\infty} d_n^{ij} x^n. \tag{35}$$

The coefficients c_n^{ij} and d_n^{ij} are obtained from the recursion relations

$$c_{n+1}^{ij}=(n+1)^{-1}\sum_{m=0}^{L+1}\sum_{j'}\left(c_{n-m}^{ij'}\left\{\left[\chi_j\binom{L}{m}-(n-m)\binom{L+1}{m+1}\right]\rho_0^{-m-1}\delta_{jj'}-\sum_{\lambda=0}^{L}\binom{L-\lambda}{m}\beta_{jj'}^{\lambda}\rho_0^{-m-\lambda-1}\right\}\right.$$
$$\left.+d_{n-m}^{ij'}\left[(\tau-t_j)\binom{L+1}{m}\rho_0^{-m}\delta_{jj'}+\sum_{\lambda=0}^{L}\binom{L-\lambda}{m}\alpha_{jj'}^{\lambda}\rho_0^{-m-\lambda-1}\right]\right),$$
$$d_{n+1}^{ij}=(n+1)^{-1}\sum_{m=0}^{L+1}\sum_{j'}\left(d_{n-m}^{ij'}\left\{\left[-\chi_j\binom{L}{m}-(n-m)\binom{L+1}{m+1}\right]\rho_0^{-m-1}\delta_{jj'}+\sum_{\lambda=0}^{L}\binom{L-\lambda}{m}\beta_{jj'}^{\lambda}\rho_0^{-m-\lambda-1}\right\}\right. \tag{36}$$
$$\left.+c_{n-m}^{ij'}\left[(\tau+t_j)\binom{L+1}{m}\rho_0^{-m}\delta_{jj'}-\sum_{\lambda=0}^{L}\binom{L-\lambda}{m}\alpha_{jj'}^{\lambda}\rho_0^{-m-\lambda-1}\right]\right)$$

with the initial conditions

$$c_0^{ij}=f^{ij}(\rho_0),\quad d_0^{ij}=g^{ij}(\rho_0). \tag{37}$$

Given the solutions of Eqs. (4) at $\rho_{\max}$, we can continue them to a point $\rho_{\max}+x$ for $x<\rho_{\max}$. Let $n(x)$ be the number of terms in the series that must be summed to attain the desired accuracy when the step size is x. In the program, x is chosen to minimize $n(x)/x$ while at the same time avoiding truncation error due to very large intermediate sums.

In this way, the solutions are continued until ρ_0 reaches or exceeds ρ_{asm} at which point the asymptotic series are evaluated and the partial wave phase shifts and amplitudes computed.

B. Summing the partial wave series

Let $\eta_R^C(\chi_j,t_j)$ be the phase shift of the regular, relativistic Coulomb wave function associated with χ_j and t_j. Also let

$$P_{fp}^{jk}=\sum_i h_{fp}^{ji}A_{fp}^{ik}\exp(i\delta_{fp}^{ik}).$$

We refer to the real numbers r_{fp}^j and ξ_{fp}^j for which $P_{fp}^{jj}=(1+r_{fp}^j)\exp\{2i[\eta_R^C(\chi_j,t_j)+\xi_{fp}^j]\}$ as the residual amplitudes and phase shifts, respectively. As f tends to infinity, the residual amplitudes and phase shifts tend to zero. ZENITH carries out the integration described above until either the residual amplitudes and phase shifts fall below a threshold ϵ specified in the program input, or f exceeds a threshold f_{last} also specified in the program input. From this point, the integration is dispensed with by setting $A_{fp}^{ij}=\delta_{ij}$ and $\delta_{fp}^{ij}=\eta_R^C(\chi_j,t_j)\,\delta_{ij}$. Additional phase shifts are accumulated in this manner until f reaches a limit specified in the program input.

Because the spherical harmonic $Y_{\lambda\mu}(\theta\phi)$ may be expressed in terms of the associated Legendre polynomial $P_\lambda^\mu(\cos\theta)$, a typical scattering amplitude may be written

$$f(\theta\phi)=\sum_\lambda a_\lambda P_\lambda^\mu(\cos\theta)\,e^{i\mu\phi}, \tag{38}$$

where the a_λ are obtained from the appropriate parts of Eq. (15). As the phase shifts and amplitudes are computed, the coefficients a_λ are accumulated for each of the scattering amplitudes. Yennie, Ravenhall, and Wilson[2] have shown that the convergence of the series (38), which may represent a function singular at $\theta = 0$, is considerably improved by the reduction

$$f(\theta\phi) = (1-\cos\theta)^{-n} \sum_\lambda a_\lambda^{(n)} P_\lambda^\mu(\cos\theta)\, e^{i\mu\phi} \tag{39}$$

in which

$$a_\lambda^{(n)} = a_\lambda^{(n-1)} - [(\lambda+1+\mu)/(2\lambda+3)]\, a_{\lambda+1}^{(n-1)} - [(\lambda-\mu)/(2\lambda-1)]\, a_{\lambda-1}^{(n-1)}, \tag{40}$$

and $a_\lambda^{(0)} = a_\lambda$. For scattering amplitudes associated with a diagonal monopole charge density, a reduction with $n = 3$ has been found necessary, while for all others, a reduction with $n = 1$ suffices.

The index λ in Eq. (38) ranges over only those orbital angular momenta for which all contributing partial waves have been computed. This implies that if $f_{\max}$ is the greatest total angular momentum for which phase shifts are computed, and I is the spin of the nucleus, then λ may not exceed $f_{\max} - I - \frac{1}{2}$. ZENITH estimates the error in the cross section due to truncation of the Legendre series from the magnitude of the last included term for each amplitude.

The computational parameters ϵ, $\Delta\rho$, $\rho_{\max}$, and $f_{\max}$, discussed in Secs. IV A and IV B are specified in the program input. The values of these and several other parameters are given in Table I for most of the runs discussed in Secs. V and VI. Since ρ_{asm} depends on f, the total angular momentum, it is given only for f_{last}, the largest value of f for which nuclear phase shifts are computed. The processing (CPU) time for each run is given in seconds for execution on an IBM 370 Model 165 computer.

C. Specification of the multipole transition densities

As discussed in Sec. III, the multipole transition density $C_\lambda(r)$ gives rise to the matrix element

$$s_\lambda(r) = [(2\lambda+1)/(4\pi)]^{1/2} \phi_\lambda(r).$$

We define the strength s_λ of the transition density $C_\lambda(r)$ to be the coefficient of $r^{-\lambda-1}$ in the asymptotic expansion of $s_\lambda(r)$. The strengths of current and magnetization transition densities are similarly defined in terms of the asymptotic behavior of the matrix elements $v_{\lambda\lambda}$ and $v_{\lambda\lambda+1}$ defined in Eq. (23).[15] ZENITH requires transition densities to be specified in terms of a strength parameter, and an unnormalized shape, which must have the form

$$F_\lambda(r) = r^\lambda \exp[-(r/a)^2] \sum_{m=0} a_m L_m^{\lambda+\frac{1}{2}}[2(r/a)^2] \tag{41}$$

in which $L_m^{\lambda+\frac{1}{2}}(x)$ is the mth generalized Laguerre polynomial of order $\lambda+\frac{1}{2}$.[16] These polynomials are orthogonal on the positive real line with weight $x^{\lambda+\frac{1}{2}} e^{-x}$. Hence any shape which behaves like r^λ near the origin and decays exponentially at infinity may be cast in this form.

For a given charge density $C_\lambda(r)$, we have

$$s_\lambda = e[4\pi/(2\lambda+1)]^{1/2} \int_0^\infty r^{\lambda+2} C_\lambda(r)\, dr \tag{42}$$

and

$$a_m = m![\Gamma(\lambda+m+\tfrac{3}{2})]^{-1} \times \int_0^\infty r^{2\lambda+2} \exp[-(r/a)^2]\, L_m^{\lambda+\frac{1}{2}}[2(r/a)^2]\, C_\lambda(r)\, dr. \tag{43}$$

The shape parameters a_m clearly depend on the

TABLE I. Computational parameters for several of the ZENITH runs discussed in the text in Secs. V and VI. The parameters are defined in Sec. IV.

Run number	E (MeV)	ϵ	$\Delta\rho$ (fm)	$\rho_{\max}$ (fm)	ρ_{asm} (fm)	$f_{\max}$ ($\frac{1}{2}\hbar$)	f_{last} ($\frac{1}{2}\hbar$)	CPU time (sec)
1	1200	7×10^{-8}	0.003	2.1	1.6	170	15	4.0
2	1200	7×10^{-8}	0.003	2.1	1.6	170	15	4.1
3	1200	7×10^{-8}	0.003	2.1	1.6	170	15	4.0
4	1200	7×10^{-8}	0.003	2.1	1.6	170	15	4.1
5	170	1×10^{-9}	0.023	13.9	15.4	170	17	4.2
6	200	1×10^{-9}	0.020	11.8	15.2	170	17	7.7
7	100	1×10^{-9}	0.010	5.9	24.8	42	42	8.0
8	100	1×10^{-9}	0.010	5.9	25.1	43	43	15.6
9	100	1×10^{-9}	0.010	5.9	25.1	43	43	15.5
10	250	1×10^{-10}	0.016	14.3	14.2	140	35	7.6
11	250	1×10^{-10}	0.016	14.3	14.2	140	35	7.6
12	250	1×10^{-8}	0.016	14.3	42.3	140	85	125.3

length parameter a. In practice, a is chosen so as to minimize the number of coefficients necessary to achieve an adequate representation of $C_\lambda(r)$. This is done in a separate input-preparation program CDFIT.

With this choice of parametrization for the transition densities, the integrals in Eq. (34) are rather easy to compute. Let coefficients b_n be chosen such that

$$\sum_{n=0}^{N} b_n (r/a)^{2n} = \sum_{n=0}^{N} a_n L_n^{\lambda+\frac{1}{2}}[2(r/a)^2] .$$

Also, let

$$I_n = a^{-2n} r^{-\lambda-1} \int_0^r x^{2\lambda+2n+2} \exp[-(x/a)^2]\, dx ,$$

$$K_\lambda = r^\lambda \int_0^r x^{2\lambda} \exp[-(x/a)^2]\, dx ,$$

and

$$J_n = a^{-2n} r^\lambda \int_r^\infty x^{2n+1} \exp[-(x/a)^2]\, dx .$$

Clearly,

$$\phi_\lambda(r) = 4\pi(2\lambda+1)^{-1} \sum_{n=0}^{N} b_n (I_n + J_n) .$$

Thus, the computation of $\phi_\lambda(r)$ may be conveniently organized as follows:

$$\phi_\lambda(r) = s_N, \quad s_n = b_n(I_n + J_n) + s_{n-1},$$

$$I_n = (\lambda + n + \tfrac{1}{2}) I_{n-1} - E_n, \quad J_n = n J_{n-1} + E_n,$$

$$E_n = (r/a)^2 E_{n-1}, \quad K_n = (n - \tfrac{1}{2}) a^2 r^{-1} K_{n-1} - F_{n-1},$$

$$F_n = r F_{n-1}, \quad s_{-1} = 0, \quad I_0 = K_{\lambda+1},$$

$$F_0 = \tfrac{1}{2} a^2 \exp[-(r/a)^2], \quad E_0 = J_0 = F_\lambda,$$

$$K_0 = \tfrac{1}{2} a \sqrt{\pi}\, \mathrm{erf}(r/a).$$

ZENITH currently allows the specification of charge and current densities, but not magnetization densities.[17]

V. TESTS OF THE PROGRAM

At the beginning of work on ZENITH, we had access to a reliable one-channel partial wave code for the scattering of electrons from spin zero nuclei when the mass of the electrons may be neglected.[3] The results of ZENITH runs on data acceptable to the older program have been found to be in agreement with results from that program to all significant digits. The tests reported here are primarily comparisons with the Born approximation in one form or another. They investigate the handling of massive projectiles, nuclei with nonzero spin, and multipole charge and current densities. In addition to these tests, it has been shown elsewhere[7] that ZENITH is in close agreement with the version of DWBA contained in the Duke program,[18] and with the DWBA program HEINEL[19] when higher order effects, which are not treated properly in DWBA, can be neglected.

In Born approximation, the differential cross section is proportional to the square of the charge z on the scattering particles. We have made four ZENITH runs (runs 1, 2, 3, and 4) in which massless particles of charge -2, -1, $+1$, and $+2$ are scattered from hydrogen nuclei ($Z = 1$, with, however, infinite mass) with a charge distribution of the form $\exp[-(\frac{1}{3}r)^2]$ at an energy of 1200 MeV. Table II displays the results for two values of the scattering angle. The tabulated functions are $(d\sigma/d\Omega)/z^2$ and its first two differences in z. Clearly, $(d\sigma/d\Omega)/z^2$ is very nearly constant. The additional differences show that even at this energy, which is quite unfavorable to the partial wave

TABLE II. $(d\sigma/d\Omega)/z^2$ and its first two differences in z at two values of the scattering angle for 1200 MeV particles scattering from infinitely massive nuclei of charge 1. The small first and second differences provide a check of ZENITH against Born approximation.

z	$(d\sigma/d\Omega)/z^2$	$\delta((d\sigma/d\Omega)/z^2)$	$\delta^2((d\sigma/d\Omega)/z^2)$
		$\Theta = 11°$	
−2	$3.929\,814\,55 \times 10^{-3}$		
		$0.005\,754\,81 \times 10^{-3}$	
−1	$3.924\,059\,74 \times 10^{-3}$		$0.000\,279\,63 \times 10^{-3}$
		$0.005\,475\,18 \times 10^{-3}$	
1	$3.913\,109\,39 \times 10^{-3}$		$0.000\,278\,64 \times 10^{-3}$
		$0.005\,196\,54 \times 10^{-3}$	
2	$3.907\,912\,85 \times 10^{-3}$		
		$\Theta = 23°$	
−2	$1.582\,519\,35 \times 10^{-4}$		
		$0.002\,351\,41 \times 10^{-4}$	
−1	$1.580\,167\,94 \times 10^{-4}$		$0.000\,194\,21 \times 10^{-4}$
		$0.002\,157\,20 \times 10^{-4}$	
1	$1.575\,853\,54 \times 10^{-4}$		$0.000\,193\,22 \times 10^{-4}$
		$0.001\,963\,98 \times 10^{-4}$	
2	$1.573\,889\,56 \times 10^{-4}$		

approach, the cross sections behave in a regular fashion.

If one performs two independent scattering experiments at the same incident momentun p, one with particles of mass m_1, the other with particles of mass m_2, then in Born approximation, the differential cross sections are in the ratio

$$\frac{(d\sigma/d\Omega)_1}{(d\sigma/d\Omega)_2} = \frac{p^2\cos^2(\frac{1}{2}\theta)+m_1^2}{p^2\cos^2(\frac{1}{2}\theta)+m_2^2}. \tag{44}$$

ZENITH has been used to compute the scattering of electrons (run 5) and also of muons (run 6) from ^{12}C. The mass of the muon was taken to be 105.66 MeV while that of the electron was neglected. The incident momentum for both computations was 170 MeV/c. Following the notation of Sec. IV C, the shape for the charge distribution had a length parameter $a = 1.77$ fm, and two nonzero shape parameters $a_0 = 1.705$ and $a_1 = -0.470$.

We see from Fig. 1 that the ratio of the cross sections as computed by ZENITH agrees with that predicted by Born approximation for small angles but falls steadily below the predicted value as the angle increases. In fact, Born approximation systematically overestimates the muon cross section relative to the electron cross section. From a classical point of view, the energy of the scattering particle, be it muon or electron, increases as it enters the nucleus. This gives rise to an increase in the momentum of the particle which is slightly greater for the muon than for the electron. As a consequence, the muon cross section is shifted to smaller angles, or equivalently, decreased at a particular angle. At 90°, Born approximation predicts a ratio of 1.773 while the ratio as computed by ZENITH is 1.670. To account for this shift when the energy gained in the nucleus is 4 MeV, the ZENITH electron cross section at 90° should actually be compared with the ZENITH muon cross section at 89.52°. The ratio of the ZENITH cross sections is then 1.771 which agrees much more closely with Born approximation.

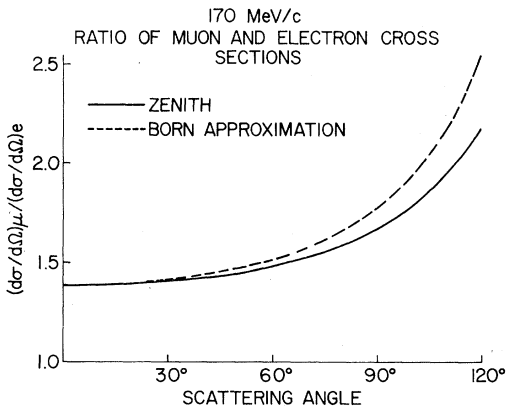

FIG. 1. The ratio of the differential cross section for muons to that for electrons as computed by Zenith and Born approximation. As explained in Sec. V, the Born approximation consistently overestimates the muon cross section relative to the electron cross section at larger angles.

The wave equation for scattering from a two-state nucleus is

$$\begin{pmatrix} H_D + V_{11} + \epsilon_1 & V_{12} \\ V_{12} & H_D + V_{22} + \epsilon_2 \end{pmatrix} \begin{pmatrix} \Psi_1 \\ \Psi_2 \end{pmatrix} = E \begin{pmatrix} \Psi_1 \\ \Psi_2 \end{pmatrix}. \tag{45}$$

As Ravenhall *et al.*[20] have shown, when $V_{11} = V_{22}$ and $\epsilon_1 = \epsilon_2 = 0$, this two-state scattering problem may be solved in terms of the two one-state scattering problems

$$(H_D + V_{11} + V_{12})\Phi_1 = E\Phi_1 \tag{46}$$

and

$$(H_D + V_{11} - V_{12})\Phi_2 = E\Phi_2. \tag{47}$$

If $f_1(\theta)$ and $f_2(\theta)$ are the scattering amplitudes for these two one-state problems, then the elastic and inelastic amplitudes for the two-state problem are given by

$$f_e(\theta) = \tfrac{1}{2}[f_1(\theta) + f_2(\theta)]$$

and

$$f_i(\theta) = \tfrac{1}{2}[f_1(\theta) - f_2(\theta)].$$

ZENITH runs corresponding to Eqs. (45), (46), and (47) show agreement with these predictions to all tabulated decimal places (in this case, nine).

Another test is provided by the observation that since a monopole charge density cannot couple different magnetic substates of the same eigenstate, scattering from a spin zero nucleus should be identical to that from a spin one-half nucleus with the same charge distributions. Comparison of ZENITH runs with spin zero and spin one-half nuclei shows agreement to six or seven decimal places. The discrepancy arises because the cutoff value for the phase shifts has a slightly different meaning for spin zero and spin one-half nuclei. (See Sec. IV B.)

Consider a nucleus with spin $I \geq \frac{1}{2}$ which is completely characterized electromagnetically by a dipole current distribution of the form

$$\vec{J}(\vec{r}) = -4v\vec{r}\exp[-(r/a)^2]/(3\pi e a^5). \tag{48}$$

The differential cross section for scattering from such a nucleus, when averaged over initial spins and summed over final spins, is given in Born approximation by

$$\frac{\overline{d\sigma}}{d\Omega} = z^2v^2(2I+1)^{-1}\exp(-q^2a^2/2)[2+\cot^2(\tfrac{1}{2}\theta)]/18,$$

TABLE III. Comparison of ZENITH and Born approximation differential cross sections for scattering of 100 MeV electrons from the pure dipole current distribution given in Eq. (48) for spin $\frac{1}{2}$ nuclei.

	Born approximation (fm^2)	ZENITH (fm^2)
1°	$9.119\,476\times10^{-1}$	$9.119\,500\times10^{-1}$
2°	$2.280\,296\times10^{-1}$	$2.280\,293\times10^{-1}$
3°	$1.013\,781\times10^{-1}$	$1.013\,777\times10^{-1}$
177°	$8.315\,185\times10^{-5}$	$8.233\,290\times10^{-5}$
178°	$8.311\,976\times10^{-5}$	$8.230\,085\times10^{-5}$
179°	$8.310\,051\times10^{-5}$	$8.228\,162\times10^{-5}$

where q is the momentum transfer and z is the charge on the scattering Dirac particle.

We have used ZENITH to compute the scattering of 100 MeV electrons from a spin one-half nucleus of this type with a strength of $v = 0.05$ fm and the length parameter $a = 1$ fm (run 7). The results for the cross sections are shown in Table III.

Finally, consider a nucleus with spin $I \geq 1$ which is completely characterized electromagnetically by a quadrupole charge distribution of the form

$$C(r) = 8\sqrt{5}\, sr^2 \exp[-(r/a)^2]/(15\pi a^7).$$

The corresponding spin-averaged differential cross section is, in Born approximation,

$$\frac{\overline{d\sigma}}{d\Omega} = 4z^2 s^2 (2I+1)^{-1} \exp(-q^2a^2/2)[E^2 - p^2\sin^2(\tfrac{1}{2}\theta)]/45 . \tag{49}$$

Columns (a) and (b) of Table IV are a comparison of Born approximation and ZENITH differential cross sections for the case $s = 0.5$ fm^2, $I = 1$, $E = p = 100$ MeV (i.e., massless projectiles), and $a = 0.25$ fm (run 8). Although the Born approximation cross section goes to zero at 180°, the ZENITH cross section does not. This is due to double-scattering higher order effects, which ZENITH computes properly. Columns (c) and (d) of Table IV are the results of a similar computation with the quadrupole strength only half as large (run 9). At 150°, the Born approximation then predicts a cross section of 3.0984×10^{-5} fm^2, while the ZENITH result is 3.1950×10^{-5} fm^2. At 179°, these become 3.5077×10^{-8} fm^2 and 9.9337×10^{-7} fm^2, respectively. Although the difference is still present, it has been greatly reduced. (It is approximately proportional to s^4, the dependence expected from an amplitude corresponding to double scattering.)

VI. ISOTOPIC VARIATIONS IN THE CHARGE DISTRIBUTION OF CALCIUM

Frosch *et al.*[21] have analyzed the scattering of 250 MeV electrons from ^{40}Ca, ^{42}Ca, and ^{44}Ca, in terms of isotopic differences in ground-state monopole charge distributions. However, because ^{40}Ca, being doubly magic, has no low-lying excited states, while ^{42}Ca and ^{44}Ca each have a low-lying 2^+ excited state, it is possible that the observed isotopic differences in differential cross sections may be due in large part to dispersion effects rather than to actual differences in the ground-state monopole charge distributions

Rawitscher[22,23] has estimated the magnitude of dispersion effects using a model in which the inelastic excitation takes place by a single *monopole* transition to a state degenerate with the ground state. The strength of this transition is adjusted to give a reasonable value for the total inelastic cross section. Applying his model to the calcium experiments referred to above, Rawitscher finds that the dispersion effects may account for as

TABLE IV. Comparison of ZENITH and Born approximation differential cross sections for scattering of 100 MeV electrons from the pure quadrupole charge distribution given in Eq. (49) for spin 1 nuclei. Columns (a) and (b) correspond to a quadrupole strength $s = 0.5$ fm^2, while columns (c) and (d) correspond to a quadrupole strength $s = 0.25$ fm^2.

	$s = 0.5$ fm^2		$s = 0.25$ fm^2	
	(a) Born approximation (fm^2)	(b) ZENITH (fm^2)	(c) Born approximation (fm^2)	(d) ZENITH (fm^2)
1°	$1.902\,450\times10^{-3}$	$1.900\,945\times10^{-3}$	$4.756\,125\times10^{-4}$	$4.734\,573\times10^{-4}$
30°	$1.774\,890\times10^{-3}$	$1.773\,220\times10^{-3}$	$4.437\,224\times10^{-4}$	$4.413\,615\times10^{-4}$
60°	$1.424\,086\times10^{-3}$	$1.422\,352\times10^{-3}$	$3.560\,214\times10^{-4}$	$3.535\,249\times10^{-4}$
90°	$9.436\,924\times10^{-4}$	$9.472\,756\times10^{-4}$	$2.359\,231\times10^{-4}$	$2.346\,484\times10^{-4}$
120°	$4.671\,357\times10^{-4}$	$4.773\,091\times10^{-4}$	$1.167\,839\times10^{-4}$	$1.171\,213\times10^{-4}$
150°	$1.239\,369\times10^{-4}$	$1.364\,838\times10^{-4}$	$3.098\,423\times10^{-5}$	$3.195\,024\times10^{-5}$
179°	$1.403\,100\times10^{-7}$	$1.254\,306\times10^{-5}$	$3.507\,750\times10^{-8}$	$9.933\,763\times10^{-7}$

much as a 5% effect in the differential cross sections in the first diffraction minimum. (The quantity quoted is actually the difference in the cross sections divided by the sum, in agreement with the usage of Frosch *et al.*) Inasmuch as the measured difference between ^{40}Ca and ^{44}Ca is on the order of 12% there, this would appear to be an important effect. This view has been emphasized by Wall.[24]

To discover if this is the case, we have computed the dispersion corrections in the ^{40}Ca-^{44}Ca case. Although the charge distributions used by Frosch *et al.* are not immediately acceptable to ZENITH, we have made fits to them that are. The resulting parameters are shown in Table V. Using these fits, we computed the elastic differential cross sections for ^{40}Ca and ^{44}Ca (runs 10 and 11). The quantity $R(\theta)$, the ratio of the difference in the cross sections to their sum is plotted in Fig. 2(a). It is in good agreement both with the experimental data and with the ^{40}Ca-^{44}Ca curve given in Fig. 8 of Ref. 21, indicating that the fitting process leading to the parameters in Table V is adequate.

We then added to the ^{40}Ca ground-state charge distribution, a 2^+ excited state coupled to the ground state by a quadrupole transition charge density (run 12). Heisenberg, McCarthy, and Sick[25] have fitted this transition charge density for ^{44}Ca. In doing so however, they treated $B(E2)$ as a variable parameter which resulted in a value for it that is different from that determined by Coulomb excitation experiments.[26] We have therefore used the Coulomb excitation value for $B(E2)$ and chosen the shape of the transition density to be that given in Eq. (1) by Heisenberg, McCarthy, and Sick. The parameters and strength for this transition density are also given in Table V. The 2^+ excited state was assumed to have a (diagonal) charge density identical to that of the ground state. The effect of the excited state on the differential cross section is shown in Fig. 2(b). The vertical scale there is *10 times larger* than that in Fig. 2(a). Although the effect grows with angle relative to the experimentally measured difference in Fig. 2(a), it remains negligible throughout the region investigated experimentally.[9] Analyses of experiments in which the ratio is sampled for larger values of the momentum transfer, however, may have to take proper account of these dispersion corrections.

Rawitscher has suggested[23] that the magnitude of the dispersion corrections may be energy dependent, growing appreciably for lower energies. We repeated the computations described above at 50 MeV. The effects are extremely small, and to within the accuracy of the computations depend only on the momentum transfer.

TABLE V. ZENITH strength and shape parameters for the calcium charge distributions used in Sec. VI. The monopole distributions were obtained by fitting to the results given in Table III of Ref. 21. The $B(E2)$ for the ^{44}Ca 2^+ state is 480 as measured in Ref. 26, and $^{44}\rho_{\text{excited}}(r) = r(d/dr)[^{40}\rho_{\text{ground}}(r)]$. For all distributions, $a = 1.99$ fm.

$^{40}\rho_{\text{ground}}$ $\lambda = 0$ $s_0^{00} = 0.145\,944$		$^{44}\rho_{\text{ground}}$ $\lambda = 0$ $s_0^{00} = 0.145\,944$		$^{44}\rho_{\text{excited}}$ $\lambda = 2$ $s_2^{01} = 0.256\,079$ fm^2	
n	a_n	n	a_n	n	a_n
0	2.309 223 5	0	2.354 695 9	0	−0.190 404 38
1	−1.388 671 3	1	−1.469 435 9	1	0.274 509 32
2	0.465 263 61	2	0.524 645 86	2	−0.191 846 41
3	−0.020 994 11	3	−0.030 256 31	3	0.032 526 47
4	−0.005 709 91	4	−0.013 376 05	4	0.019 039 94
5	−0.021 036 00	5	−0.022 613 65	5	0.005 532 25
6	0.000 093 475	6	−0.001 853 795	6	−0.005 044 521
7	0.002 158 589	7	0.003 543 130	7	−0.003 907 150
8	0.002 788 878	8	0.003 182 487	8	−0.001 408 490

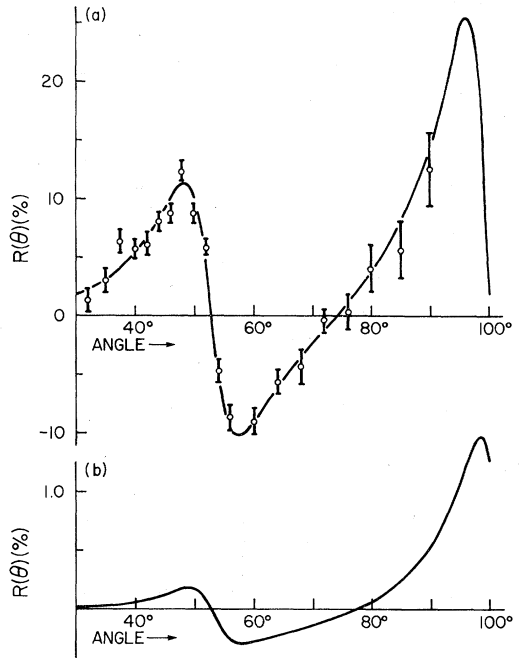

FIG. 2. The ratio, $R(\theta) = [^{40}\sigma(\theta) - ^{44}\sigma(\theta)] / [^{40}\sigma(\theta) + ^{44}\sigma(\theta)]$, is plotted as a function of scattering angle. (a) The ^{44}Ca cross section is computed using the ground-state monopole charge distribution determined by Frosch *et al.* (Ref. 21) as fitted by us with the parameters shown in Table V. The experimental data are from Table II b of Ref. 21. (b) The ^{44}Ca cross section is computed using the ^{40}Ca ground-state charge distribution and a 2^+ excited state coupled to it, as described in Sec. VI. Note that the vertical scale is 10 times greater than that in (a).

VII. SUMMARY AND DISCUSSION

ZENITH obtains for the scattering of a Dirac particle from a nucleus, a numerical solution which is exact to the extent that the nucleus may be treated as a nonrelativistic object possessing a finite number of degenerate energy eigenstates coupled to one another through the electromagnetic interaction with the Dirac particle. The most vexing of these limitations is the requirement that the eigenstates be degenerate in energy unless the corresponding radial wave equations decouple asymptotically. The need for this restriction arises because we have been unable to produce usable recursions for the coefficients of the asymptotic series when $k_i \neq k_j$ in Eq. (9).

The program has been designed to allow direct access to the scattering amplitudes defined in Eq. (15), thus making it quite easy to treat scattering from polarized or aligned nuclei[7] and to compute such things as the polarization of the scattered particles.

Although we have developed the computational scheme presented here for the Dirac equation in the presence of the electromagnetic field of the nucleus, the key ingredients to its practical success (i.e., the asymptotic solution of the coupled radial wave equations discussed in Sec. II, and the analytic continuation of the radial wave equations by power series expansions as described in Sec. IV A) are applicable to more general scattering situations. As was mentioned in Sec. I, Saladin, Roesel, and Alder[8] have suggested a very similar method for the Schrödinger equation. We have verified that ZENITH works well in the nonrelativistic domain associated with Coulomb excitation. We are in the process of developing a program similar to ZENITH for particles satisfying the Klein-Gordon equation.

Interactions other than the electromagnetic interaction may be used simply by evaluating the matrix elements corresponding to those in Eqs. (20) and (21) and placing them properly in Eqs. (4). Complex potentials have been added to an earlier version of ZENITH for use in optical model calculations,[27] and we are currently adding them to ZENITH itself. Thus ZENITH offers the potential for handling, in a single program, scattering situations ranging from very low energies all the way up to energies at which strong interactions in the form of an optical model potential may be treated.

ACKNOWLEDGMENTS

This work was begun when the author was a graduate student at the University of Illinois under the advisorship of D. G. Ravenhall whose enthusiastic support has been an invaluable aid to its completion. The author acknowledges the support of a National Science Foundation Graduate Fellowship during this period.

---

*Supported in part by the National Science Foundation under Grant No. NSF-GP-25303. Based on work submitted in partial fulfillment of the requirements of the degree of Doctor of Philosophy in the Computer Science Department of the University of Illinois.

[1]An extensive bibliography of the history of electron scattering computations is given by H. Überall, *Electron Scattering from Complex Nuclei* (Academic, New York, 1971).

[2]D. R. Yennie, D. G. Ravenhall, and R. N. Wilson, Phys. Rev. 95, 500 (1954).

[3]R. Herman, B. C. Clark, and D. G. Ravenhall, Phys. Rev. 132, 144 (1963), describe a program which is based on that of Ref. 2.

[4]J. M. McKinley, Phys. Rev. 183, 106 (1969).

[5]D. G. Ravenhall, in *Proceedings of the International Conference on Photonuclear Reactions and Applications, 1973*, edited by B. L. Berman (Lawrence Livermore Laboratory, Livermore, 1973), Vol. 1, p. 30.

[6]R. L. Mercer and D. G. Ravenhall, Phys. Rev. C 10, 2002 (1974).

[7]D. G. Ravenhall and R. L. Mercer, Phys. Rev. C 13, 2324 (1976).

[8]J. X. Saladin, F. Roesel, and K. Alder, Bull. Am. Phys. Soc. 21, 12 (1976), Abstract AE7. We thank Professor Saladin for private discussion concerning their method.

[9]Although the present work includes the low lying collective transitions, it does not include transitions to the high lying giant resonances and, as such, does not give a complete account of the dispersion corrections.

[10]R. L. Mercer, Ph.D. thesis, Department of Computer Science, University of Illinois, 1972 (unpublished).

[11]We choose units for which $\hbar$ and c are dimensionless and numerically equal to unity.

[12]For Clebsch-Gordan coefficients and Wigner 3-J, 6-J, and 9-J symbols, we use the standard phase conventions as defined, for example, in Appendix C of A. Messiah, *Quantum Mechanics* (North-Holland, Amsterdam, 1966), Vol. II.

[13]In practice, $k_i^2 - k_j^2$ is often quite small which causes the recursion to be numerically bad. This fact has made it necessary for us to assume degenerate the energy eigenvalues of nuclear states for which the radial wave equations do not decouple asymptotically.

[14]Although $\vec{J}^T$ may be expressed as the sum of a current density and the curl of a magnetization density in infinitely many ways, there is exactly one choice which allows both the current density and the magnetization density to be expressed as sums which include only the vector spherical harmonics $\vec{X}_{\lambda\mu}$. When chosen in this way, $\vec{J}^C(\vec{r})$ accounts entirely and solely for transverse

magnetic excitations, while $\vec{\mu}(\vec{r})$ contributes to transverse electric excitations. Our $\vec{J}^C(\vec{r})$ is identical to $\vec{j}_0^{\,op}(\vec{r})$ as defined by Überall, Eq. (4-21e) in Ref. 1.

[15]In terms of the matrix elements $B(C\lambda)$ and $B(M\lambda)$, we have

$$s_\lambda = \pm e^2[4\pi B(C\lambda)(2I+1)/(2\lambda+1)]^{1/2}$$

and

$$v_{\lambda\lambda} = \pm e^2[4\pi B(M\lambda)(2I+1)(\lambda+1)/\lambda]^{1/2},$$

where I is the spin of the initial nuclear state. The ambiguity in the sign, which arises because $B(C\lambda)$ and $B(M\lambda)$ involve nuclear matrix elements squared, may be resolved by the choice of a particular nuclear model.

[16]M. Abramowitz and I. A. Stegun, *Handbook of Mathematical Functions with Formulas, Graphs, and Mathematical Tables* (National Bureau of Standards, Washington, 1964), Series 55.

[17]See footnote 14.

[18]The Duke program is described by S. T. Tuan, L. F. Wright, and D. S. Onley, Nucl. Instrum. Methods 60, 70 (1968).

[19] HEINEL is a program, based on the Duke program, written by J. Heisenberg, mentioned in Ref. 25.

[20]D. G. Ravenhall, D. R. Yennie, B. C. Clark, and R. Herman, Nucl. Phys. 72, 177 (1965).

[21]R. F. Frosch *et al.*, Phys. Rev. 174, 1380 (1968).

[22]G. H. Rawitscher, Phys. Rev. 151, 846 (1966).

[23]G. H. Rawitscher, Phys. Lett. B33, 445 (1970).

[24]N. S. Wall, Ann. Phys. 66, 790 (1971).

[25]J. H. Heisenberg, J. S. McCarthy, and I. Sick, Nucl. Phys. A164, 353 (1971).

[26]M. Bini *et al.*, Nuovo Cimento Lett. 5, 913 (1972).

[27]The resulting program, CNADIR, has been used, for example, in B. C. Clark, *et al.*, Phys. Rev. C 7, 466 (1973).